

Energy-aware co-optimization of facility layout and AGV configuration in intelligent manufacturing cells

Xin Wang^{a,b}, Huiyu Zhang^{a*}, Jianjun Liu^a, Qingxin Chen^a and Zhenwei Li^a

^aGuangdong University of Technology, Key Laboratory of Computer Integrated Manufacturing Systems, Guangdong, China

^bFoshan University, Management School Guangdong, China

CHRONICLE

Article history:

Received January 8 2026
Received in Revised Format
March 31 2026
Accepted March 18 2026
Available online March 18
2026

Keywords:

Loop layout
Intelligent manufacturing cells
Energy consumption
Joint optimization
Non-dominated classification
genetic algorithm

ABSTRACT

In order to meet the market demands for customization and rapid response while controlling carbon emissions in manufacturing systems, it has become increasingly important to consider the collaborative optimization of equipment layout in smart production units alongside intelligent storage and transportation systems. This study investigates the loop layout problem of smart manufacturing units equipped with Automated Guided Vehicles (AGVs) through a novel simulation-optimization framework integrating intelligent search algorithms with directed graph-based isomorphism detection. An optimization model is presented with the objective functions of maximizing production capacity and minimizing energy consumption, constrained by performance indicators such as relative position of the equipment within the unit, AGV transport speeds and buffer capacity. Given the lack of a closed mathematical expression for this multi-objective function, a second-generation NSGA-II based on simulation is designed to solve the model. Furthermore, a method based on directed graph isomorphic layout processing is proposed to quickly eliminate similar solutions, enhancing solution quality and algorithm efficiency. Through comparative experimental design and practical applications in intelligent workshops, the effectiveness, superiority, and application value of this optimization algorithm in addressing the circular layout problem of smart production units are validated.

© 2026 by the authors; licensee Growing Science, Canada

1. Introduction

The manufacturing sector accounted for approximately 90% of industrial electricity consumption, making energy efficiency improvement a critical challenge for mitigating energy demand and associated emissions. In conventional manufacturing systems, machine tools-as fundamental energy-consuming components- have been systematically classified, designed and evaluated for energy conservation purposes (Schudeleit et al., 2016; Zhou et al., 2016). However, the transition to smart manufacturing introduces new energy considerations, particularly with the integration of Automated Storage and Transportation System(ASTS) like automatic guided vehicles (AGVs). These advanced systems are projected to substantially increase overall energy and resource demands.

While current research extensively explores joint configuration and scheduling optimization for energy reduction(Yue et al., 2019; Bányai, 2023), a more holistic approach incorporating energy efficiency considerations during early-stage factory planning needs to be developed. For facilities undergoing smart manufacturing transformation, such proactive integration can simultaneously enhance production capacity while achieving significant energy savings. The facility layout design is a fundamental aspect of production system management, where the optimal allocation of facilities to particular designated locations, known as the facility layout problem(FLP)-directly impacts system efficiency and effectiveness(Amar & Abouabdellah, 2016; Kubalik et al., 2023; Koren, 2019). Modern FLP must address:

- (1) Dynamic Layout Requirements: With reconfigurable manufacturing systems (RMS) enabling flexible capacity, layouts must adapt to intelligent manufacturing cells (IMCs) combining machines, buffers, and AGVs(Fragapane et al., 2022).
- (2) AGV-Integrated Optimization: While loop layouts are widely adopted in IMCs, existing Loop Layout Problem(LLP)

* Corresponding author

E-mail hyzhang_henry@126.com (H. Zhang)

ISSN 1923-2934 (Online) - ISSN 1923-2926 (Print)

2026 Growing Science Ltd.

doi: 10.5267/j.ijiec.2026.3.011

formulations fail to incorporate AGV allocation strategies and energy consumption metrics, despite their critical role in IMCs where speed/buffer configurations affect congestion

- (3) Multi-Phase Integration: Only 4% of studies address both block/detailed layouts (Pérez-Gosende et al., 2021), though smart manufacturing requires simultaneous optimization of intelligent units and ASTS integration (Mittal et al., 2019; Shang et al., 2025).

Our proposed method addresses these gaps by:

- (1) Incorporating AGV status (not just paths) in layout optimization.
- (2) Establishing energy consumption limits as a multi-objective (Tayal et al., 2017; Ferretti et al., 2023).
- (3) Unifying traditionally phased approaches for cellular layouts (Ye and Zhou, 2007; Zhao et al., 2020).

The optimization of intelligent equipment layout, which aims to balance production capacity and energy consumption, falls under the domain of multi-objective optimization problems (MOPs). In recent decades, multi-objective evolutionary algorithms (MOEAs) have gained significant popularity owing to their capability of efficiently identifying multiple Pareto-optimal solutions while retaining practical operational details (Ma et al., 2023). Among the wide range of MOEA variants, the non-dominated sorting genetic algorithm-II (NSGA-II), introduced by Deb et al. (2002), stands out as a widely recognized benchmark. Subsequent research has sought to enhance the original NSGA-II framework by addressing its limitations and improving its applicability to real-world scenarios. For instance, Li and Li (2023) presented a hybrid method integrating NSGA-II with tabu search (TS) to optimize a multi-row layout model that also considers automated guided vehicle (AGV) routing. TS is used to improve Since the evolution process of NSGA-II is easily hampered when facing multi-objective problems. Therefore, this study proposes an integrated optimization method--the Intelligent Cell with AGV-based Loop Layout Problem (ICALLP)--that simultaneously considers AGV dispatching status and energy consumption. In the ICALLP framework, workstations and I/O buffers are strategically arranged along a unidirectional loop track to optimize workpiece transport efficiency; AGV velocity profiles and buffer capacities are co-optimized with layout parameters to ensure workstation coordination; Energy consumption is explicitly modeled as a function of AGV movement dynamics and idle time. The remainder of the paper is structured in the following manner: Section 2 provides a critical review of existing research on the FLP of intelligent units and AGV delivery systems, highlighting their limitations in adapting to dynamic and environmentally sustainable contexts. Section 3 outlines the foundational assumptions and formally defines the loop layout problem under consideration. In Section 4, a simulation-based solution framework is established, along with a system performance evaluation model designed to support the simulation. Additionally, an enhanced version of the NSGA-II is introduced, incorporating an isomorphic layout processing mechanism to accelerate convergence. Section 5 details a case study that demonstrates the application of the proposed method, along with results from a corresponding numerical experiment. Finally, Section 6 offers concluding remarks and summarizes the contributions of the paper.

2. Literature review

2.1. Facility Layout Problem

The material flow variability categorizes FLP into two groups: static facility layout problem (SFLP) with stable material flows, and dynamic facility layout problem (DFLP) with time-varying flows (Drira et al., 2007). For SFLP, establishing lower bounds through departmental arrangements remains fundamental, typically modeled via the quadratic assignment problem (QAP) framework (Loiola et al., 2007). As an NP-hard combinatorial optimization problem (Johnson & Garey, 1979) with exponential complexity growth (Castillo & Peters, 2004; Drira et al., 2007), SFLP solutions increasingly adopt multi-objective approaches integrating: 1) Simulation techniques (Lin & Sharp, 1999; Azadivar & Wang, 2000; Wang et al., 2008; Jithavech & Krishnan, 2010); 2) Heuristic algorithms (Azadivar & Wang, 2000; Singh & Sharma, 2006; Samarghandi et al., 2010; Erik & Kuvvetli, 2021); 3) Metaheuristics (Zhang et al., 2009; Derakhshan & Wong, 2017; Erik & Kuvvetli, 2021). Production uncertainty transforms SFLP into DFLP when material flows exhibit temporal variations across multiple periods (Rezazadeh et al., 2009; Kheirkhah et al., 2015). Two primary factors govern DFLP complexity: Facility characteristics and Material handling system (MHS) configurations (Pérez-Gosende et al., 2021). Digital transformation emphasizes MHS optimization, where layout patterns (single-row, multi-row, loop, etc.) directly impact mathematical modeling. Smart manufacturing units particularly require integrated optimization of: equipment layouts, automated guided vehicle (AGV) systems and Energy-efficient robot movements. Solution methodologies for DFLP have developed greatly in the past two decades. Mathematical programming dominates DFLP research, with models addressing: problem representation, objective function formulation, demand uncertainty and data type constraints. Solution approaches mirror SFLP methods but require enhanced computational efficiency (Urban, 1998). Metaheuristics provide robust frameworks, including: 1) Particle swarm optimization (Derakhshan & Wong, 2017; Mohammed & Hasan, 2017); 2) Genetic algorithms (Dunker et al., 2005; Zarea Fazlelahi et al., 2016; Erik & Kuvvetli, 2021); 3) Ant colony optimization (Chen & Rogers, 2009; Chen & Lo, 2014); 4) Hybrid methods (Zha et al., 2020; Zouein & Kattan, 2022). In dynamic environment, system performance are difficult to calculate, simulation model integrated with heuristics or metaheuristics can find the optimum layout satisfying the multi-objectives more efficiently (Azadivar & Wang, 2000; Azimi & Saberi, 2013; Pourhassan & Raissi, 2017; Peng et al., 2018).

2.2. AGVs and FLP

As material handling equipment, including conveyors and automated guided vehicles (AGV), becomes increasingly sophisticated and energy-intensive, researchers have demonstrated that integrated layout and material handling system design yields superior results compared to traditional sequential approaches (Erik & Kuvvetli, 2021). Traditional two-phase methodologies that address layout and MHS design separately typically produce suboptimal solutions when compared to simultaneous optimization strategies (Sedehi & Farahani, 2009). Emerging strategies include: mixed integer programming for joint layout/aisle design (Klausnitzer & Lasch, 2019), virtual reality-assisted planning (Phoon et al., 2017), and energy-aware AGV routing (Yao et al., 2024; Zhang et al., 2024).

2.3. Energy Efficiency and FLP

Energy efficiency considerations have become increasingly critical in modern manufacturing systems. Transportation operations accounts for 38% of total manufacturing energy consumption (Liu et al., 2019). Systematic optimization during initial design phases offers substantially greater energy reduction potential compared to operational adjustments alone. Incorporating energy efficiency considerations during the design phase of both production systems and their associated transportation infrastructure enables more impactful optimization, achieving superior results with reduced implementation effort (Nguyen et al., 2026). The inherent conflict between production capacity maximization and energy consumption minimization in intelligent manufacturing cells necessitates novel algorithmic approaches for effective DFLP resolution.

2.4. Multi-objective Problem in FLP

The optimization of intelligent equipment layouts considering dual objectives of production capacity and energy consumption represents a classic multi-objective optimization problem (MOP). In recent years, multi-objective evolutionary algorithms (MOEAs) have gained considerable attention for their effectiveness in identifying a set of Pareto-optimal solutions while maintaining practical relevance in real-world settings (Ma et al., 2023). Among various MOEA approaches, NSGA-II remains one of the most widely recognized and applied methods. Subsequent research has sought to refine the NSGA-II framework to overcome its limitations and improve its applicability. For example, Durmaz and Sahin (2017) utilized NSGA-II to address the single-row facility layout problem, aiming to reduce total flow distance while enhancing closeness ratings. Guo et al. (2023) further adapted NSGA-II to determine layout configurations in an unequal-area facility layout context, considering both material handling costs and closeness scores in an air-conditioner manufacturing environment. Zhao et al. (2020) improved the classical NSGA-II by a new selection operation to solve cell manufacturing FLP with the goal of minimizing the area and logistics handling volume. Facing diverse layout configurations and optimization objectives in static facility layout problems, researchers have pursued two primary directions: developing improved standalone or hybrid algorithms, and applying these algorithms to dynamic facility layout problems in increasingly intelligent manufacturing environments.

2.5. Hybrid Simulation for FLP

A hybrid methodology integrating the NSGA-II with TS was developed by Li and Li, (2023) for addressing multi-row layout optimization that incorporates AGV routing. Meanwhile, Pourhassan and Raissi, (2017) utilized NSGA-II to find the optimal facility layout under rearrangement scenarios, using simulation to assess transporter interference. Huo et al. (2021) introduced an enhanced NSGA-II equipped with an adaptive local search operator, aiming to minimize total movement distance while maximizing closeness rating scores. NSGA-II has demonstrated significant popularity in both SFLP and DFLP applications with multiple objectives, and shows enhanced capability when modified or hybridized with simulation methods or other heuristic algorithms that incorporate unique environmental details. While existing studies have extensively investigated multi-objective optimization in manufacturing systems, critical gaps remain in addressing the joint optimization of equipment layout and robot speed in intelligent cells with ring-based configurations. Prior works predominantly focus on isolated objectives, either throughput maximization or energy minimization, while neglecting their inherent trade-offs. Furthermore, conventional NSGA-II implementations fail to account for topological isomorphism in ring layouts, resulting in redundant computational overhead during evolution.

The research contributions of this paper are:

- (1) **Isomorphism-Aware optimization:** In loop-based facility layouts, mutation operations frequently produce isomorphic solutions, structurally distinct layouts that yield identical system performance metrics. Proactive elimination of these isomorphic individuals prevents redundant computation for functionally equivalent solutions, significantly accelerating the overall optimization process. Leveraging directed graph theory, we introduce a post-mutation isomorphism detection mechanism to eliminate symmetric duplicates in ring layouts;
- (2) **Hybrid Simulation Optimization:** A hybrid simulation optimization framework integrates Plant Simulation with NSGA-II for accurate performance evaluation under stochastic conditions with finite buffers and resource constraints. It jointly optimizes equipment layout and robotic movement speed to enhance manufacturing cell productivity while reducing

energy consumption. While layout affects AGV travel distance, speed impacts both efficiency and energy use. NSGA-II operates like a Genetic Algorithm but overcomes key limitations of the first-generation NSGA, lack of elitism, parameter-dependent diversity maintenance, and high computational complexity, by introducing fast non-dominated sorting, a crowding distance operator, and elitist strategies. The simulation model evaluates post-mutation individuals to retain operational realism, though its lengthy runtime requires computational efficiency improvements.

(3) A decoupled encoding strategy employing mixed-variable representation to separate discrete layout variables from continuous speed parameters, enabling specialized crossover and mutation operators for each variable subspace.

These advances collectively address the unresolved challenge of efficiently deriving non-dominated solutions for layout-speed co-optimization in stochastic, resource-constrained production systems.

3. Problem formulation

The intelligent production unit is an organizational form of the production unit in an intelligent factory, incorporating two key production functions, material processing and material storage and transportation, more compactly. The equipment within the unit is generally arranged around the outer side of a circular track for robot movement. As shown in Fig. 1, in an intelligent production unit, m workstations are connected by an AGV running on a loop, workpieces are entering this unit from the pick-up buffer and exiting from the download buffer. Specifically, the material processing subsystem consists of multiple workstations such as stamping machines, processing centers, CNC machine tools, and quality inspection machines. The material storage and transportation subsystem is made up of robots for automatic loading and unloading, along with storage buffers. The intelligent production unit formed by these two subsystems can achieve functions such as processing automation, material transportation automation, automatic changing of fixtures and tools, as well as monitoring and inspection automation.

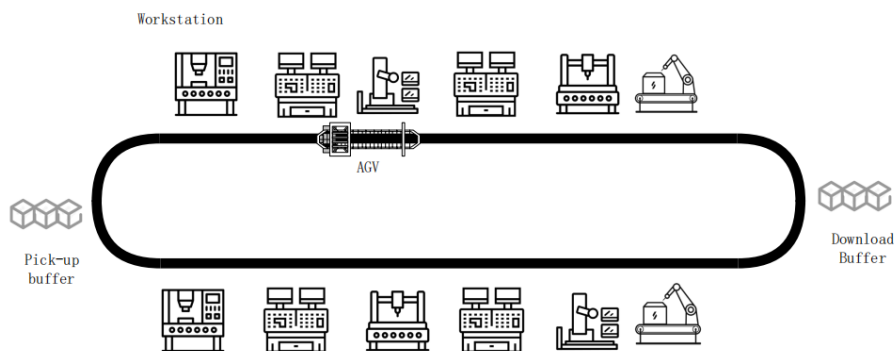


Fig. 1. An example of AGV-based Intelligent Manufacturing Unit

3.1. System assumption

The operation process within the intelligent unit is coordinated by three types of resources: workstations, transporting AGV, and storage buffers. This creates resource collaboration constraints, meaning that insufficient capacity in any resource type can lead to system inefficiencies due to blocking and waiting. Transporting AGV follows a "first come, first served" rule for service requests and exhibits three working states: idle, unladen movement, and laden movement. If the AGV arrives at a workstation with a full storage buffer and cannot unload, it will wait, potentially causing a deadlock in the intelligent unit.

The intelligent production unit satisfies the following assumptions:

- (1) The process of transporting workpieces from external areas to the unit's loading port is not considered; workpieces are prepared in advance and can be directly selected at the loading port;
- (2) When workpieces arrive from outside the unit, they are temporarily stored in the loading buffer, waiting for the AGV to transfer them to the first processing workstation;
- (3) Each workstation has only one machine that can process only one workpiece at a time; workpieces arriving must wait in the front buffer, when the workstation is busy;
- (4) After processing at the workstation, workpieces are temporarily stored in the rear buffer, waiting for the AGV to transfer them to the next workstation until all processes are completed, at the finishing point, products are transported by the AGV to the unit's download buffer before leaving the unit;
- (5) The AGV's capacity is one and can only transport one workpiece at a time; AGV is considered to move in a straight line while cruising on the track;
- (6) All buffers can store multiple workpieces.

Factors such as machine failures and workpiece rework, which may cause sudden production disturbances, are not considered.

3.2. Problem statement

The intelligent manufacturing cell loop layout problem (IMCLLP) under consideration is defined by a non-linear mathematical programming formulation with integer decision variables, where the notation is introduced as follows:

X	facility layout vector, $X = \{x_{ij}\}$, decision variables; $x_{ij} = 1$ if facility i is on location j , otherwise is 0; $i, j = 1, 2, \dots, n$.
v	cruising speed of AGV.
θ	Throughput rate of the unit
E	Energy assumption of the unit.
n	The number of facilities in the unit, including pick-up and download buffers.
t	the simulation duration
E_s	Total energy consumption of the AGV for a single task.
E_{am}	Energy consumption of the AGV during the acceleration phase.
E_{um}	Energy consumption of the AGV during the cruising phase.
E_a	Additional energy consumption from other energy-consuming components.
P_a	Power of energy-consuming components.
t_{idle}	Idle time of the AGV.
t_{ac1}	The acceleration time when the AGV cannot reach cruising speed while moving from position p to position q . $p, q = 1, 2, \dots, n$.
t_{ac2}	The time required to accelerate from 0 to cruising speed.
t_{de1}	The deceleration time when the AGV moves from position p to position q .
t_{de2}	The time required to decelerate from cruising speed to 0.
t_{pq}	Total time of AGV from position p to position q .
c_1	The AGV load status, loading is 1, otherwise is 0.
c_2	The AGV speed status, 1 is the speed reaching, otherwise is 0.
l_z	Total cruising distance.
l_{pq}	The cruising distance from position p to position q .
l_{ac}	The accelerating distance.
l_{de}	The decelerating distance.
η	Energy efficiency factor.
F_t	Driving force.
F_f	Frictional force.
f	Frictional force.
g	Gravitational acceleration.
a_{ac}	Acceleration.
a_{de}	Deceleration.

In the IMCLLP problem, performance indicators of the production system, such as production capacity and energy consumption, are difficult to express using closed-form mathematical formulas (Zhang et al., 2025). Therefore, a simulation model will be used to obtain these values, which will serve as the fitness values for individuals in subsequent optimization algorithms. While the production capacity can be calculated relatively easily in a plant simulation experiment, yielding more reliable results, the estimation of the AGV's energy consumption warrants further exploration.

The AGV is battery-driven and often starts and stops while performing transportation tasks in the unit. As a result, the actual energy consumption is inevitably higher than that of a constant speed operation. Estimating AGV energy consumption solely based on uniform-speed operation is inadequate. Therefore, the energy consumption of AGV transportation includes both loaded and unloaded transportation energy consumption.

The calculation methods of the performance indicators of the intelligent unit mentioned in this article are shown as follows.

$$\max \theta(X, v) \quad (1)$$

$$\min E(X, v) \quad (2)$$

subject to

$$\sum_{i=1}^n x_{ij} = 1, \forall j \quad (3)$$

$$\sum_{j=1}^n x_{ij} = 1, \forall i \quad (4)$$

$$v_{\min} \leq v \leq v_{\max} \quad (5)$$

$$\theta = \frac{\text{num}(X, v)}{t} \quad (6)$$

$$E = \sum_{i=1}^n E_s^i + P_a t_{idle} \quad (7)$$

$$E_s = E_{am} + E_{um} + E_a \quad (8)$$

$$E_{am} = \frac{F_t l_{ac}}{\eta} \quad (9)$$

$$E_{um} = (1 - c_2) \frac{F_f l_z}{\eta} \quad (10)$$

$$E_a = P_a t_{pq} \quad (11)$$

$$F_t = m_{total} a_{ac} + F_f \quad (12)$$

$$F_f = f m_{total} g \quad (13)$$

$$m_{total} = m_1 + c_1 m_2 \quad (14)$$

$$l_z = l_{pq} - l_{ac} - l_{de} \quad (15)$$

$$l_{ac} = \frac{1}{2} c_2 a_{ac} t_{ac2}^2 + \frac{1}{2} (1 - c_2) a_{ac} t_{ac2}^2 \quad (16)$$

$$l_{de} = c_2 (v_{ac} t_{de1} - \frac{1}{2} a_{de} t_{de1}^2) + (1 - c_2) (v_{de2} - \frac{1}{2} a_{de} t_{de2}^2) \quad (17)$$

Eq. (1) and Eq. (2) define the optimization objectives as the maximization of the total number of finished workpieces and the minimization of energy consumption, respectively. These objectives are achieved by determining the optimal vehicle allocation vector and the appropriate AGV speed. Eq. (3) and Eq. (4) together specify that each position can host only one device, and each device can be assigned to only one position. Eq. (5) defines the configurable range of the AGV cruising speed.

The system performance evaluation model is formulated in Eq. (6) to Eq. (17). The production organization method of the intelligent unit is encapsulated in a simulation black box, as simulation experiments are more suitable for capturing the characteristic behaviors of such units and enable a more accurate evaluation of the objective function values. Accordingly, the simulation model is established based on the performance evaluation framework outlined in this section. Eq. (6) defines the throughput rate of the unit, which denotes the simulation duration and represents the total output during. Eq. (7) gives the total energy consumption of the AGV. Eq. (8) expresses the energy consumed during a single AGV movement, which consists of the energy during acceleration, cruising, and the energy used by other power-consuming components. Eq. (9) to Eq. (11) provide the calculation methods for the acceleration phase energy consumption, cruising phase energy consumption, and the energy consumption of other components, respectively. Eq. (12) and Eq. (13) describe the computation of driving force and frictional force. Eq. (14) defines the total weight calculation. Eq. (15) to Eq. (17) specify the formulas for calculating the AGV movement distances at different stages. The coupling relationship between throughput rate and energy consumption poses significant challenges for both problem modeling and solution. The facility layout optimization problem is a typical combinatorial optimization problem in which the search space grows exponentially with the number of devices. When integrated with the AGV speed optimization, the resulting multi-objective problem, aiming to maximize throughput and minimize energy consumption, exhibits high nonlinearity and non-convexity. Although converting one objective into a constraint can simplify the model into a single-objective form and reduce computational complexity, multi-objective optimization allows for the simultaneous consideration of multiple goals, thereby mitigating excessive reliance on any single objective. By identifying the Pareto optimal set, this approach enhances the robustness and stability of the optimization results. Therefore, this paper adopts the joint objectives of maximizing the production capacity of intelligent units and minimizing the energy consumption of AGVs.

In the context of the IMCLLP problem, key performance indicators of the production system, such as production capacity and energy consumption, are difficult to express in closed-form mathematical formulas. Hence, a simulation model is employed to estimate these values, which subsequently serve as fitness values for individuals in the optimization algorithm. While production capacity can be reliably evaluated through plant simulation experiments, accurately estimating AGV energy consumption requires further analysis. AGVs are battery-powered and frequently start and stop during transportation tasks within the unit. As a result, their actual energy consumption is inevitably higher than under constant-speed operation. Estimating AGV energy consumption based solely on uniform-speed conditions is therefore inadequate. Accordingly, the energy consumption associated with AGV transportation must account for both loaded and unloaded travel conditions.

4. Enhanced NSGA-II algorithm with isomorphism processing

As described in Section 3.2, the IMCLLP problem is defined as a multi-objective nonlinear integer programming problem. NSGA-II (Non-Dominated Sorting Genetic Algorithm II) is an improved algorithm based on the core processes of Genetic Algorithms (GA) for multi-objective optimization problems. The original NSGA (first generation Non-Dominated Sorting Genetic Algorithm) has an efficient way to solve multi-objective optimization problems by using heuristic methods, but it

also has shortcomings: 1) lacks an elite individual retention mechanism; 2) primarily relies on experience to maintain population distribution during iterations; 3) The time complexity of constructing the non-dominated solution set using non-dominated sorting is high. Therefore, this paper introduces improvements such as fast non-dominated sorting, crowding comparison operator, and elite strategy.

4.1. Encoding and decoding

The genetic algorithm requires the design of encoding rules. In this paper, the individual encoding is composed of the concatenation of equipment layout information encoding and AGV speed information encoding, as shown in Fig. 2.

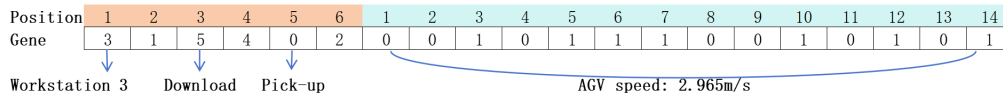


Fig. 2. Schematic diagram of individual encoding

The encoding of equipment layout information is on the left side of the gene. The code width corresponds to the problem scale. If there is positions on the outer edge of a circular track, the equipment layout information code is represented as a n -dimensional array that can accommodate loading ports (P), unloading ports (D), and $n-2$ workstations. The set of workstations is denoted as $\{S_1, S_2, \dots, S_{n-2}\}$. For example, for a problem scale of 6, $n=6$, with 6 positions that need to be allocated to 4 workstations and a pair of P/D ports, the relationship array can be represented as $\{S_3, S_1, D, S_4, P, S_2\}$. This array indicates that in this layout scheme, position 1 is allocated for workstation S_3 , position 2 is for S_1 , position 3 is for the unloading port, and and so on. For convenience in calculations, the loading port is represented as 0, the unloading port as $n-1$, and workstations are encoded from 1 to $n-2$. The equipment layout encoding for this scheme is represented as $[3, 1, 5, 4, 0, 2]$. The AGV speed information encoding is on the right side of the gene. Currently, the speed of AGVs used for transportation in the workshop is generally set between 0 and 3 m/s. To ensure experimental accuracy, three decimal places are retained, such as 2.965 m/s. Therefore, a 14-bit binary encoding is used, which, when converted to decimal, has a value range of $[0, 8192]$. For example, the binary 00101110010101 converts to decimal 2965. Dividing by 1000 gives the AGV's speed value. In summary, by combining the equipment layout information encoding and the AGV speed information encoding, an individual encoding is formed, with the encoding length depending on the problem scale. Additionally, in applying crossover and mutation operations during the merging process, traditional actions should be adjusted to ensure the correctness of the encoded information.

4.2. Population initialization

The initial population is generated by randomly creating equipment layout information encoding and AGV speed encoding, then concatenating them to form individuals' encoding. The population size is set to 70, with a three-point crossover operation at a ratio of 0.8, and a single-point mutation operation at a ratio of 0.2.

4.3. Fitness value

Performance indicators of the production unit, such as capacity and energy consumption, are estimated through simulation experiments. Due to the randomness inherent in smart units, such as the uncertainty of order arrival times, variability in processing sequences and requirements for incoming workpieces, and unpredictability of AGV transport cycles, it is challenging to compute performance metrics using closed-form mathematical formulas. The results from these formulas may not accurately reflect actual production scenarios. Therefore, it is necessary to utilize simulation techniques with strong detail capabilities for modeling, combined with scientific experimental design, to provide more reliable data and validate the key factors influencing system performance. This article uses Tecnomatix Plant Simulation 15.0 software to establish a simulation experimental platform, operating in a PC Windows 10 environment, with hardware consisting of an Intel(R) CPU at 2.50GHz and 12.0GB RAM. A simulation model of an intelligent production unit with AGV circular transportation is established, as shown in Fig. 3.

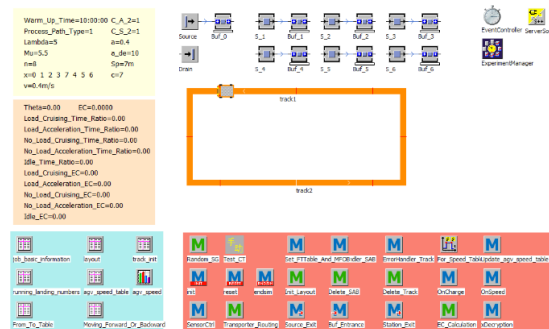


Fig. 3. Diagram of the simulation model with AGV circular transportation.

4.4. Directed graph-based isomorphism detection

The AGV path planning problem can be expressed by using graph theory: define a directed graph $D=(V', A')$ to describe the AGV's movement paths, with the vertex set $V'=\pi, \text{to} \forall \pi(p), \pi(q) \in V'$, the two-element pair $\pi(p), \pi(p)$ represents the reachable paths of the AGV, and the set of reachable paths constitutes A' , the arc set of the directed graph. The isomorphic property of directed graphs refers to the existence of two directed graphs, a and b, that have the same topological properties, which remain preserved even after performing specific set transformations.

For the circular layout problem of intelligent units, the randomly generated layout information encoding may appear different, but they share the same topological properties. This means that there are different layout encodings that express the same layout. There are four types of isomorphic layouts in this study:

- (1) Central rotational isomorphism. For encoding $x_1 = \{1, 2, \dots, p - 1, p, p + 1, \dots, n\}$, randomly select an element p from it and use p as the first element to recode, and the new encoding result $x_2 = \{p, p + 1, \dots, n, 1, 2, \dots, p - 1\}$ is isomorphic to x_1 , as shown in Fig. 4(a);
- (2) Vertex axis of symmetry inversion isomorphism. The encoded sequences x_1 and x_2 have the same length n . If n is an even number and $q=n/2$, for $\forall p \in [1, q]$, let $x_2(p) = x_1(q + p)$, which means that the elements at the p^{th} position and the $(q + p)^{th}$ position are swapped. After the swap, the encoded sequence x_2 is isomorphic to x_1 , as shown in Figure 4(b);
- (3) Arc axis of symmetry inversion isomorphism. The encoded sequences x_1 and x_2 have the same length n . If n is an even number and $q=n/2$, for $\forall p \in [0, q - 1]$, let $x_2(1 + p) = x_1(n - p)$, which means that the elements at the $(1 + p)^{th}$ position and the $(n - p)^{th}$ position are swapped. After the swap, the encoded sequence x_2 is isomorphic to x_1 , as shown in Fig. 4(c);
- (4) Vertex-arc axis of symmetry inversion isomorphism. The encoded sequences x_1 and x_2 have the same length n . If n is an uneven number and $k=\lfloor n/2 \rfloor$, for $\forall p \in [0, \lfloor n/2 \rfloor]$, let $x_2(k + p) = x_1(k - p)$, which means that the elements at the $(k + p)^{th}$ position and the $(k - p)^{th}$ position are swapped. After the swap, the encoded sequence x_2 is isomorphic to x_1 , as shown in Fig. 4(d).

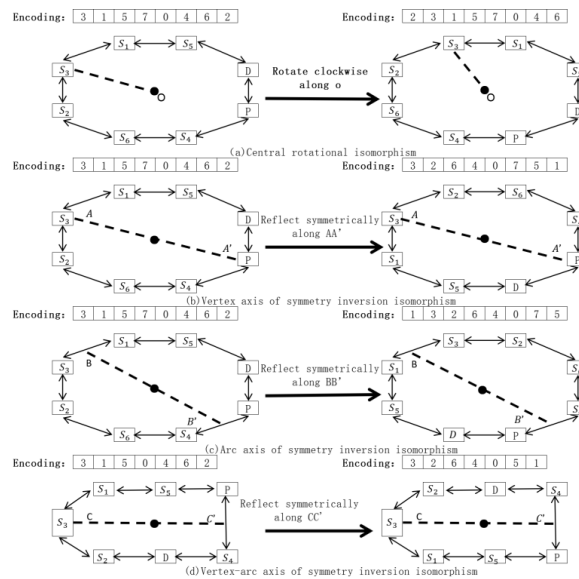


Fig. 4. Layout Encoding and Isomorphic Topology Diagram

Fig. 4 shows the correspondence between isomorphic encoding and isomorphic layout. The 0 in the layout encoding represents P in the isomorphic layout, and the maximum value in the layout encoding represents D in the isomorphic layout. The remaining numbers correspond to workstation numbers, such as 3 corresponding to S_3 and 1 corresponding to S_1 in the encoding. This paper considers both the equipment layout and AGV speed. During the evolutionary process, if the layout encodings of two random individuals are isomorphic and the speed values obtained from their speed encodings differ by a small amount, as defined by $V \in (V_p - \epsilon, V_p + \epsilon)$, and $p=1, 2, \dots, n$, $V_1 - \epsilon \geq V_{min}$, $V_n + \epsilon \leq V_{max}$, where ϵ is a sufficiently small value, these two random individuals can be considered as 'isomorphic individuals'. By removing isomorphic individuals before calculating the fitness value, the running time of the algorithm can be significantly reduced.

4.5. Crossover and mutation operations

Considering that the equipment layout encoding must ensure the uniqueness of the genes in the chromosome, meaning each

gene should appear only once in the chromosome, the Partially-Matched Crossover (PMX) operator is more suitable. However, the chromosome for the speed encoding part does not need to follow the uniqueness principle. Therefore, in this paper, based on the traditional two-point PMX crossover operator, an additional crossover point is introduced specifically for the speed encoding part, as shown in Fig. 5. That is, two crossover points are randomly generated in the equipment layout encoding part, and one crossover point is randomly generated in the speed encoding part. The encoding between the first and second crossover points, as well as the encoding after the third crossover point, are exchanged. After the exchange, a uniqueness check is performed.

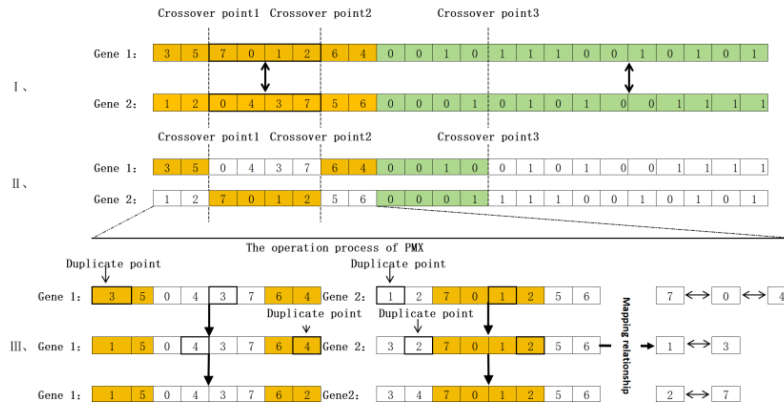


Fig. 5. Operation Process of Partial-mapped Crossover

4.6. Fast non-dominated sorting genetic algorithm

In the IMCLLP problem, production system performance indicators such as capacity and energy consumption are difficult to express using closed-form mathematical formulas. Therefore, a simulation model will be used to obtain these values, which will serve as the fitness values of individuals. Since there are multiple conflicting fitness values, direct comparison and selection cannot be performed in the genetic algorithm. To address this issue, NSGA-II introduces the fast non-dominated sorting rule.

The non-dominated sorting rule refers to constructing a set of non-dominated solutions based on the dominance relationships between solutions, and then ranking the remaining solutions by their levels. Individuals with higher ranks are selected to enter the next generation. However, when there are too many individuals in a particular rank, random selection may not easily produce elite individuals, leading to a longer search time. Therefore, to accelerate the selection process of non-dominated sorting, this paper introduces the concept of crowding distance as a rule for selecting elite individuals, embedding it within the non-dominated sorting procedure to shorten the algorithm's search time.

The dominance (Dominate) relationship is used in multi-objective optimization to compare the quality of two solutions. When a solution A is said to dominate another solution B , denoted as $A < B$, it means that A is no worse than B in all objectives and strictly better than B in at least one objective. This relationship satisfies two conditions: 1) For all sub-objectives, A is no worse than B , $f_k(A) \leq f_k(B)$ ($k=1,2,\dots,r$), r represents the number of sub-objectives; 2) There exists at least one sub-objective such that A is strictly better than B , for $\exists l \in 1,2,\dots,r, f_l(A) < f_l(B)$.

At this point, the solution is called non-dominated, or non-inferior, or non-dominated, while B is said to be dominated. If there are multiple solutions that do not dominate each other, their combined performance is considered relatively superior, forming a non-dominated set. Before the selection operation, it is necessary to construct the non-dominated set and rank the other individuals outside this set. An iterative algorithm is employed, as outlined below.

1: Non-dominated Sorting Algorithm

1.1: Set $A=1$

1.2: Set $B=A+1$

1.3: calculate the objective values of A -th and B -th individuals in the population, and compare the objective values: if $A > B$, $A.dominanceSet = A.dominanceSet \cup \{B\}$ (Record B in A 's dominance set), and $B.dominated = B.dominated + 1$ (Increment B 's dominated count by 1); else if $B.dominanceSet = B.dominanceSet \cup \{A\}$ (Record A in B 's dominance set), $A.dominated = A.dominated + 1$ (Increment A 's dominated count by 1).

1.4: rank the individual's dominated counts: if $A.dominated=0$, then add A to first rank set $F\{1\}$.

1.5: let $A=A+1$, proceed to step 1.4. When $A=length(pop)$, proceed to step 2.

2: Classify individuals into ranks (excluding first rank)

2.1: Set $rk=1$

2.1 To individual A in the first rank set, Select individual A' from $A.dominanceSet$, let $A'.dominated=A'.dominated-1$, if $A'.dominated=0$, $A'.rank=rk+1$, and then put A' into rank set $F\{rk+1\}$;

2.2 Set $rk=rk+1$, and classify the new rank's individuals, then generate the next rank's individuals, until there's no individuals dominated counts is 0; stop the iteration.

To accelerate non-dominated sorting while ensuring the distribution and diversity of the population, this paper introduces the

concept of crowding distance as a supplementary rule for ranking individuals, giving priority to individuals with larger crowding distances. The crowding distance formula (18) defines the crowding distance of an individual as the sum of the differences in objective function values between the individual and its neighboring individuals. First, the non-dominated set is constructed, and the crowding distance of each individual is calculated. Then, the individuals are sorted in ascending order based on the levels derived from the non-dominated set, and within the same level, individuals are sorted in descending order of their crowding distance.

$$pop(a).distance = \sum_{k=1}^r |pop(a+1).f_k - pop(a-1).f_k| \tag{18}$$

4.7. Selection operation

The fast non-dominated sorting assigns all individuals from both the parent and offspring populations to corresponding ranks based on dominance and non-dominance relations. A certain proportion of individuals are then selected to enter the next generation population. First, individuals from higher non-dominated ranks are selected. When all individuals from a certain rank cannot enter the next generation at the same time, individuals with larger crowding distances are chosen to enter the next generation. The selection operation is shown in Fig. 6, where P_t represents the parent population, Q_t represents the unselected offspring population after crossover and mutation, and F_1, F_2, \dots, F_{r_k} represent the various ranks, P_{t+1} denotes the new population.

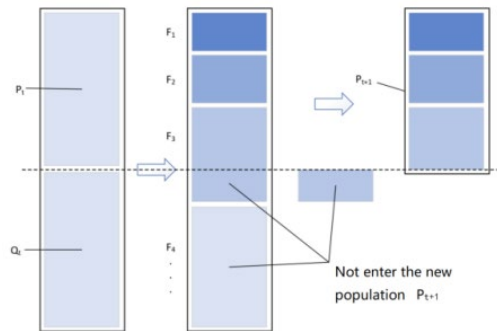


Fig. 6. NSGA-II Selection Operation

4.8. Algorithm process

This paper employs an improved NSGA-II algorithm. For the randomly generated initial population, a three-point crossover operation is applied to the gene encoding in segments, based on PMX. After crossover, a single-point mutation operation is performed on the offspring. Once the correctness check is passed, the parent and offspring populations are merged. The merged population is then traversed to identify isomorphic individuals, marking one individual from each isomorphic group. The fitness value of this marked individual is calculated using a simulation model, and this fitness value is shared with the other isomorphic individuals, thus reducing the number of simulation model calls and shortening the solution time. Then, the fast non-dominated sorting rule is applied to select elite individuals to enter the next generation population. The algorithm process is shown in Fig. 7.

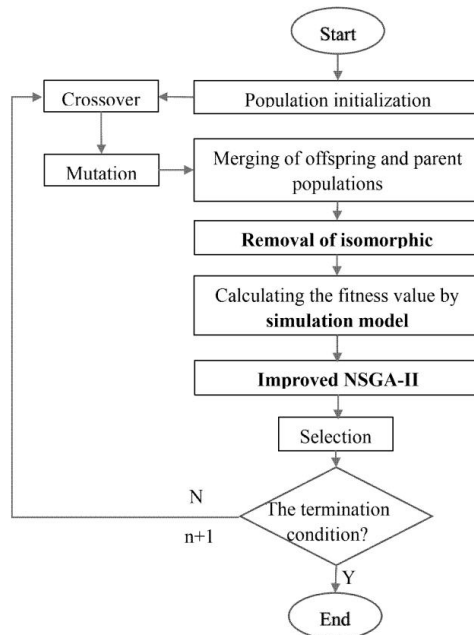


Fig. 7. Algorithm Process

5. Computational experiments and results

5.1. Experiment design

This paper designs 12 test cases, considering factors such as: number of devices (6-8 units), process path types (serial and serial-parallel), arrival and processing rates, AGV speed, buffer capacity, and so on. The experimental case parameters are shown in Table 1. λ represents the workpiece arrival rate; μ represents the processing rate; N represents the buffer capacity; C_A^2 is the squared coefficient of variation for the input process distribution; C_S^2 is the coefficient of variation for the processing (service) process, and Sp is the equipment position spacing. The simulation runtime for each experiment is set to 500 days, with a warm-up time of 10 hours. Each test case is conducted for 100 experiments, and the performance metric values obtained are averaged to serve as the simulation results.

Table 1
Experiments for Comparison of Different Process Path Types and Operations

Test Number	Process path type and operations	λ	μ	C_A^2	C_S^2	N	Sp
1	Serial 0-3-5-4-2-6-1-7	5	5.5	1	1	7	7
...
12	Serial parallel 0-6-7-1-5-8-3-9 0-2-4-1-5-8-3-9	5.5	4	1	0.5	15	6

5.2. Simulation experiment on performance influencing factors

(1) Equipment layout experiment

The equipment layout experimental results show that in the intelligent unit layout, as the distance between the loading and unloading ports gradually decreases, the capacity increases while the energy consumption decreases. As shown in Figure 8, regardless of whether the workstations are arranged in serial processes or serial-parallel processes, the performance results indicate that the examples can be classified into three types: capacity-energy consumption optimization combination, capacity-energy consumption deterioration combination, and capacity-energy consumption isomorphic combination. In the capacity-energy consumption optimization combination, the capacity increases while the energy consumption decreases. Specifically, as shown in Fig. 8(a) for the serial process of 6 workstations, the layout series of examples from 6A1 to 6A4 are [0,1,2,3,7,4,5,6], [0,1,2,3,4,7,5,6], [0,1,2,3,4,5,7,6], and [0,1,2,3,4,5,6,7]. Here, 0 represents the loading port, 7 represents the unloading port, and 1,2,3,4,5,6 represent the workstations arranged in sequential order according to the process. Due to the circular layout, whether 0 and 7 appear at the two ends of the array or are placed adjacent to each other within the array, they are effectively positioned next to each other in the actual layout, forming a circular connection. As can be seen from the figure, as the unloading port 7 moves closer to the loading port 0, the capacity increases while the energy consumption shows a downward trend. At the same time, for the example series from 6A5 to 6A7, the layouts are [0,1,2,4,7,3,5,6], [0,1,3,4,7,6,2,5], and [0,1,5,3,7,4,2,6]. In this case, when the distance between the loading and unloading ports remains large and unchanged, disrupting the sequential order of the workstations' processes results in increasingly undesirable capacity and energy consumption performance, thus leading to a capacity-energy consumption optimization outcome.

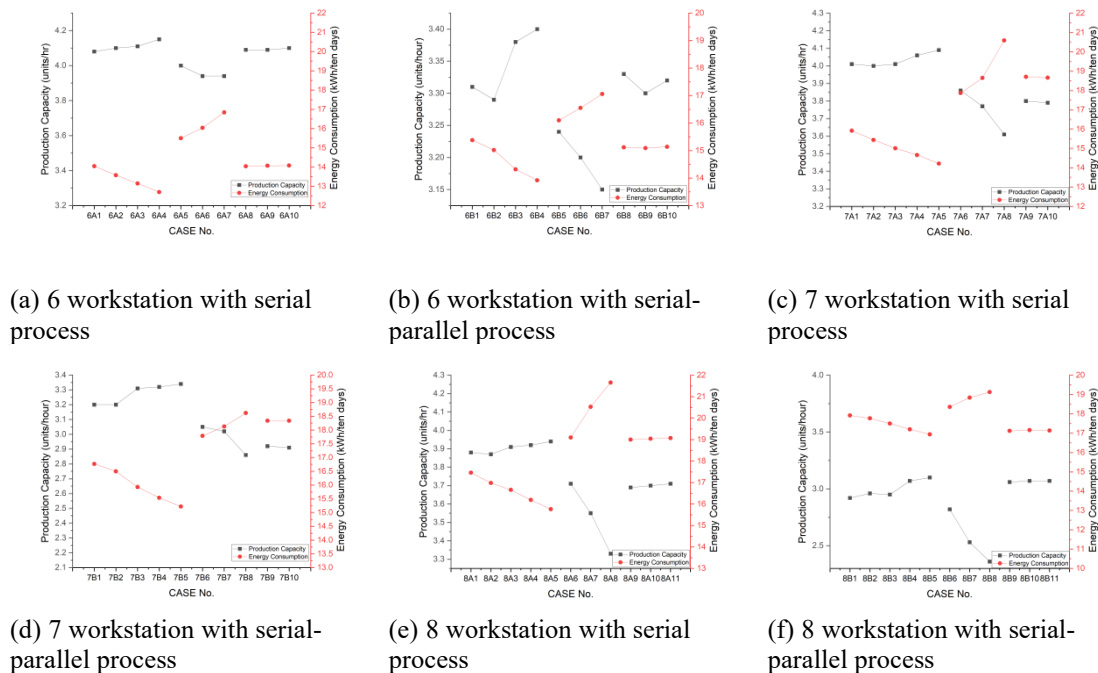


Fig. 8. Throughput-energy Tradeoffs under Different Layout Configurations

It is worth noting that in the examples where the loading and unloading ports are kept at a large and fixed distance, even if the workstations are not arranged in a sequential order, the capacity and energy consumption remain unchanged. This phenomenon is referred to as an isomorphism in the layout, but it is not the optimal solution, thus forming a capacity-energy consumption isomorphic combination. From the series of examples shown in Fig. 8, it can be seen that the correlation between these three capacity-energy consumption indicators and the layout also applies when the number of workstations is increased. Notably, as the number of workstations increases, cases where the workstations are arranged in process order show better performance in both energy consumption and capacity indicators. Therefore, in intelligent unit layouts, workstations should be arranged as closely as possible in process order, and the relative positions of the unit’s loading and unloading ports should be kept as close as possible.

(2) AGV moving speed experiment

When the number of workstations remains constant, the robot’s movement speed is positively correlated with capacity within a certain range. Once the robot’s speed reaches a certain value, further increases in speed will no longer significantly enhance the production unit’s capacity. The robot’s movement speed is positively correlated with energy consumption over a wide range, and increasing speed will consistently lead to higher energy consumption. As shown in Fig. 9 (a) and Fig. 9(b), when the number of workstations remains constant, regardless of whether the process path is serial or serial-parallel, as the AGV speed increases, the capacity will shift from growth to small fluctuations around a certain value θ_1 , which is slightly higher than the range of [0.4, 0.7] for the serial-parallel process. As the AGV speed continues to increase, after reaching a larger value v_2 , the maximum energy consumption is E_1 . In all experiments, $v_1 < v_2$, therefore, the AGV speed v_1 which achieves the highest capacity is also the speed that results in the lowest energy consumption under the given experimental conditions.

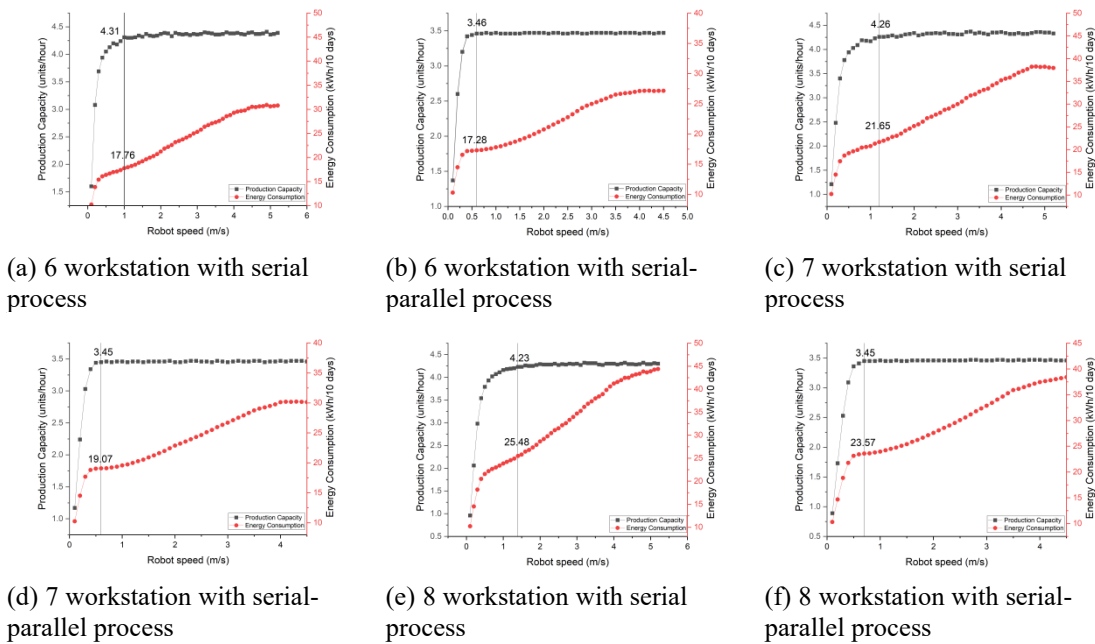


Fig. 9. Robot Moving Speed Experiment

(3) Work intensity experiment

The work intensity of the intelligent unit is highly positively correlated with both capacity and energy consumption within a certain range. As shown in Fig. 10, with the increase in work intensity, both capacity and energy consumption also increase. When the work intensity reaches a certain threshold, the performance indicators almost simultaneously reach their maximum values and no longer increase. Under fixed workstation numbers and layout, the upper limit of the unit's work capacity is fixed. When the work intensity is below the unit’s work capacity, capacity increases, and energy consumption rises with the actual consumption of equipment and transportation. However, when the work intensity reaches or even exceeds the unit’s work capacity, the capacity and energy consumption of the fully loaded intelligent unit reach their limits and no longer increase, but there is severe clogging of workpieces both inside and outside the unit.

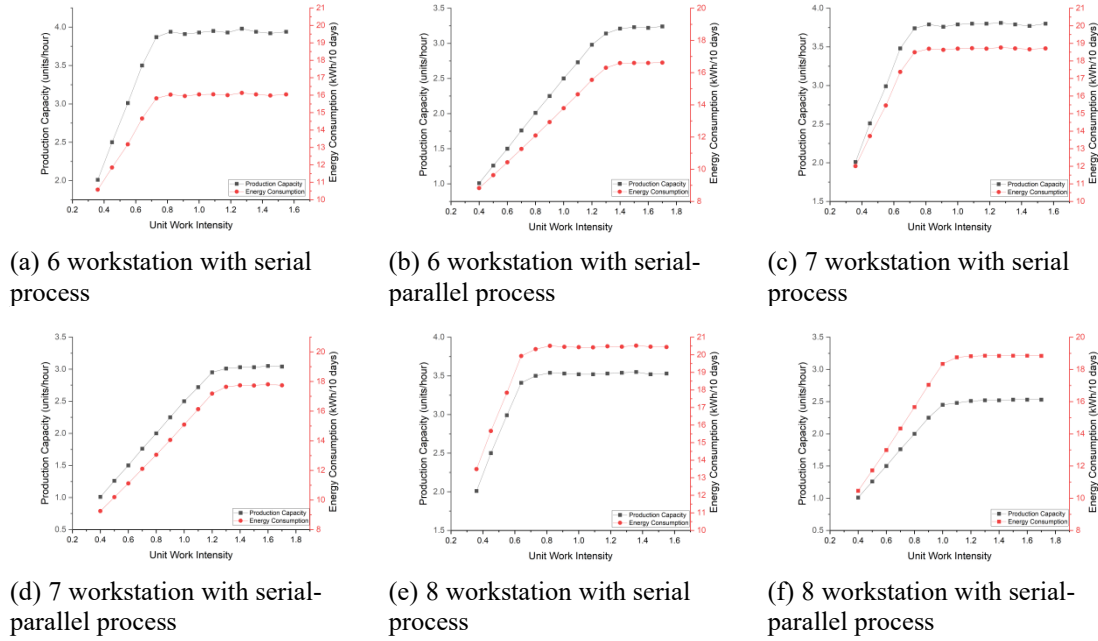


Fig. 10. Unit Work Intensity Experiment

(4) Buffer capacity experiment

When the workstation layout and process type are determined, adding a buffer zone and increasing its capacity will simultaneously increase both capacity and energy consumption. However, when the buffer zone capacity reaches a certain threshold, both capacity and energy consumption will reach their maximum values and no longer change significantly, as shown in Figure 11. It is worth noting that under serial process conditions, the effect of increasing buffer zone capacity on capacity is more significant for units of different sizes. For serial-parallel processes, as the number of workstations increases, the effect of increasing buffer zone capacity on capacity becomes less noticeable. In simple terms, for intelligent units under serial process conditions, setting a buffer zone with a certain capacity can effectively improve the unit's capacity.

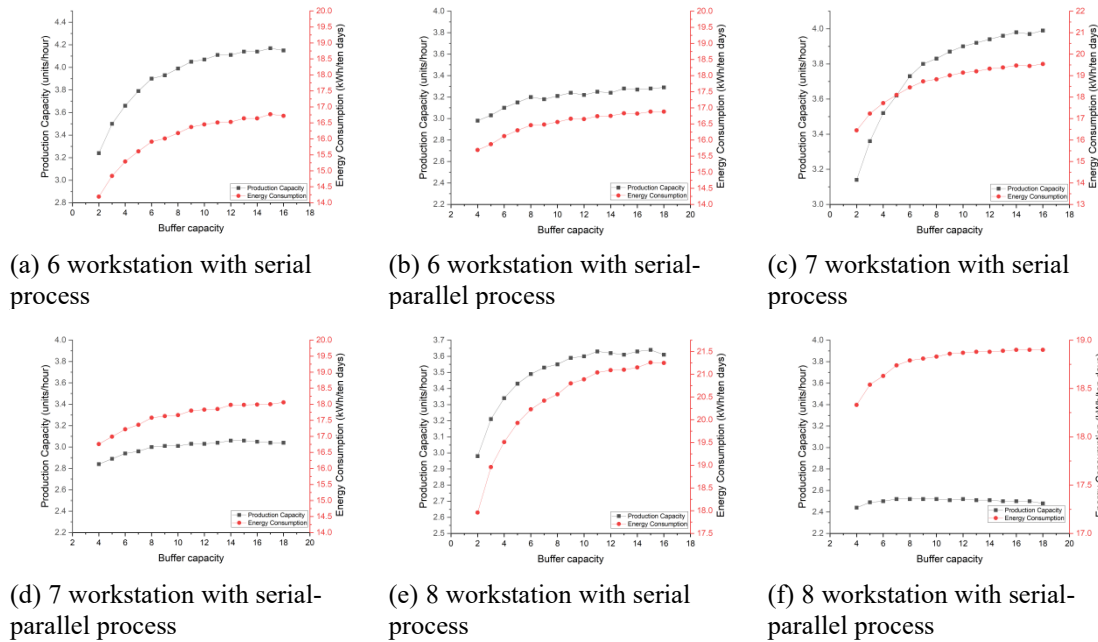


Fig. 11. Buffer Zone Capacity Experiment

5.3. Selection of comparison algorithms

In this paper, the Migratory Bird Optimization (MBO), Ant Colony Optimization (ACO), and NSGA-II algorithms are used as comparison algorithms to validate the effectiveness of the directed graph-based isomorphic processing improvement in genetic algorithms. The details of the comparison algorithms and the relationship matrix diagram of the comparison points are shown in Table 2. Among them, the bird swarm size for MBO is 51, with each bird exploring 3 solutions in the search domain, 1 shared solution, and each leader bird making 3 rounds of exploration. The iteration termination condition is when

more than 2000 domain solutions are explored. For ACO, the ant swarm size is 50, the pheromone evaporation coefficient is 0.2, and the maximum number of iterations is 30. The objective function values for MBO and ACO are obtained by linearly weighting and summing the capacity and energy consumption, with a weight ratio of 6:4.

Table 2
Comparison of Optimization Algorithms

Algorithm	Characteristics
Migratory Bird Optimization (MBO)	Demonstrated effectiveness in solving complex optimization problems
Ant Colony Optimization (ACO)	Notable for its computation time efficiency in path-finding problems
Non-dominated Sorting Genetic Algorithm II (NSGA-II)	Provides superior solving performance through embedded fast non-dominated sorting approach
Improved NSGA-II (INSGA-II)	Proposed enhancement that reduces computation time by 30% compared to standard NSGA-II

5.4. Comparative Analysis

(1) Comparison of computation time

Regardless of changes in problem scale, process path types, or buffer capacity, the average computation time of the improved NSGA-II algorithm is significantly lower than that of the MBO and ACO algorithms. In most test cases, it is slightly better than the NSGA-II algorithm. This indicates that the improvement by eliminating isomorphic individuals can effectively reduce the algorithm's computation time.

(2) Comparison of population distribution

The diversity of the solution set is one of the important indicators for evaluating multi-objective algorithms, meaning that the non-dominated individuals in the obtained solution set should be evenly distributed across the entire solution space. In this paper, the grid distribution degree evaluation method is used to compare the performance of various algorithms. The distribution degree ranges from [0,1], with a higher value indicating better diversity of the solution set. The computation process is as follows:

- ① Select the non-dominated set $F^{(t)}$ from the population $P^{(t)}$, where $F^{(t)}$ is non-dominated with respect to P^* .
- ② For each grid i, j, \dots , calculate $H(i, j, \dots)$ and $h(i, j, \dots)$ using the following two equations:

$$H(i, j, \dots) = \begin{cases} 1, & \text{if the grid contains an individual } X (X \in P^*) \\ 0, & \text{else} \end{cases} \tag{19}$$

$$h(i, j, \dots) = \begin{cases} 1, & \text{if } H(i, j, \dots) = 1 \text{ and an } X \text{ in the grid } (X \in P^*) \\ 0, & \text{else} \end{cases} \tag{20}$$

$$D(P^{(t)}) = \frac{\sum_{h(i, j, \dots) \neq 0}^{i, j, \dots} m(h(i, j, \dots))}{\sum_{H(i, j, \dots) \neq 0}^{i, j, \dots} m(H(i, j, \dots))} \tag{21}$$

- ③ For each grid, calculate the value of $m(h(i, j, \dots))$ based on $h(i, j, \dots)$ and the values of $h()$ of its neighboring grid. Similarly, calculate $m(H(i, j, \dots))$ based on the values of $H()$ in the reference set.
- ④ Calculate the distribution function by averaging the values of $m(h(i, j, \dots))$ and $m(H(i, j, \dots))$.

As shown in Fig. 12, the distribution degree of the solution sets obtained by NSGA-II and the improved NSGA-II is higher than that of MBO and ACO in all 12 test cases. Meanwhile, the distribution degree of NSGA-II is higher than that of the improved NSGA-II, which is influenced by the presence of isomorphic individuals.

(3) The score of the solution set

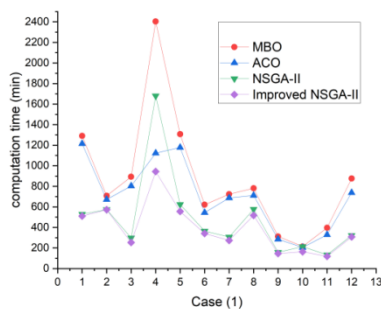


Fig. 12. Comparison of Algorithm Computation Time

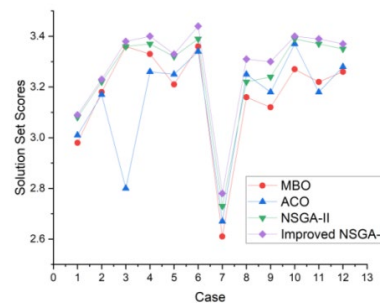


Fig. 13. Comparison Chart of Solution Set Scores

To comprehensively evaluate each algorithm, the score of the solution set is calculated, and the calculation process is shown in Eq. (22).

$$QScore = \frac{a + 4b + 8c}{16 popNum} + 1.75d \quad (22)$$

where a represents the number of remaining individuals after removing isomorphic individuals; b represents the distribution score of the solution set after removing isomorphic individuals, i.e., the $m(H(i,j,...))$ related to Eq. (19); c represents the distribution score of the non-dominated individuals in the solution set after removing isomorphic individuals, i.e., the $m(h(i,j,...))$ related to Eq. (20); and d represents the maximum value of the weighted capacity and energy consumption of all individuals in the solution set after removing isomorphic individuals. Eq. (22) reflects both the number of solutions and the diversity of the solution set after removing isomorphic individuals. The larger the QScore value, the better the quality of the solutions in the set. Fig. 13 shows that the solution set scores of the improved NSGA-II are higher than those of other algorithms that do not remove isomorphic individuals in all test cases, clearly demonstrating that removing isomorphic individuals leads to a higher quality solution set.

6. Industrial case validation

An automotive parts manufacturing enterprise produces a wide range of components covering transmissions, engines, and chassis systems. Its main products include bearing cap assemblies, input/output shafts, oil filter bracket assemblies, differential housings, and output flanges. The manufacturing process of these components involves various types of equipment, such as lathes, boring machines, milling machines, drilling machines, machining centers, CNC lathes, and testing equipment. The manufacturing processes of these components are shown in Table 3. For clarity in representation, the production processes for each component can be expressed as numerical sequences shown in Table 4.

Table 3
Part Manufacturing Processes

Part	Operation No.	Operation Name	Equipment
Bearing Cap	1	Drilling	Vertical Drill/Z5140
	2	Chamfering	Milling Machine/X8130A
	3	Riveting	Riveting Press
	4	Surface Milling	Milling Machine/X8130A
	5	Facing	Lathe/CAK3665Ni
	6	Deburring	Bench Vise
	7	Inspection	Inspection Bench
Input&Output Shaft	1	Rough Turning	Lathe/CAK3665Ni
	2	Drilling	Vertical Drill/Z5140
	3	Facing	Lathe/CK6140A
	4	Boring&Reaming	Machining Center
	5	Finish Turning	Lathe/CAK3665Ni
	6	Deburring	Bench Vise
	7	Surface Milling	Milling Machine/X51
Bracket	8	Inspection	Inspection Bench
	1	Hole Enlargement	Bench Drill/Z4112
	2	Surface Milling	Milling Machine/X8130A
	3	Tapping	Bench Tapping Machine/S4012B
	4	Hole Enlargement & Burnishing	Machining Center
	5	Drilling	Vertical Drill/Z5140
	6	Deburring	Bench Vise
Differential Case	7	Inspection	Inspection Bench
	1	Rough Turning	Lathe/CA6140
	2	Finish Turning	Lathe/CAK3665Ni
	3	Rough Filing	Filing Machine/T618
	4	Boring & Reaming	Machining Center
	5	Tapping	Vertical Drill/Z5140
	6	Inspection	Inspection Bench
Output Flange	1	Turning	Lathe/CA6140
	2	Drilling	Vertical Drill/Z5140
	3	Cylindrical Grinding	Grinding Machine/M1432B
	4	Inspection	Inspection Bench

Table 4
Production Process Sequences for Components(Coded Representation)

No.	Component Name	Process Sequence
1	Bearing Cap Assembly	1-2-3-2-4-5-6
2	Input/Output Shaft	4-17-8-4-5-9-6
3	Oil Filter Bracket Assembly	10-2-11-8-1-5-6
4	Differential Housing	12-4-13-8-1-6
5	Output Flange	12-1-14-6

Note: Equipment codes correspond to: 1-Z5140, 2-X8130A,3-Riveting Press, 4-CAK3665Ni, 5-Bench Vise, 6-Inspection Bench, 7-CK6140A, 8-Machining Center, 9-X51, 10-Z4112, 11-S4012B, 12-CA6140, 13-T618, 14-M1432B.

Taking the production of the aforementioned automotive components as an example, an improved NSGA-II algorithm was employed to solve both equipment layout schemes and robot velocity configurations in the smart manufacturing cell for these five parts. The NSGA-II parameters were configured as follows: population size=100, generations=40, crossover probability=0.8, and mutation probability=0.2. The top ten Pareto-optimal solutions are presented in Table 5.

Table 5
Non-dominated Solutions for layout-Velocity Co-optimization

No.	Layout Strategy	Robot Speed (m/s)	Throughput (units/h)	Energy (kWh)
1	[10,8,13,15,6,1,3,11,14,2,0,7,5,12,9,4]	3.41	6.03	30.44
2	[6,4,14,9,15,13,3,8,2,7,10,12,0,1,11,5]	0.29	0.27	6.26
3	[13,15,6,5,9,0,4,12,3,10,2,7,1,8,11,14]	2.72	6.00	23.11
4	[13,15,6,5,9,0,4,12,10,3,2,7,1,8,11,14]	0.90	5.99	16.17
5	[13,15,6,5,9,0,4,12,3,10,2,7,1,8,11,14]	0.40	5.27	14.56
6	[15,7,14,11,9,2,10,13,3,0,12,4,8,1,5,6]	0.67	5.54	14.59
7	[15,7,14,11,9,2,10,13,3,0,12,4,8,1,5,6]	0.50	4.91	13.65
8	[15,7,14,11,9,2,10,13,3,0,12,4,8,1,5,6]	0.40	3.63	11.50
9	[13,15,6,5,9,0,4,12,3,10,2,7,1,8,11,14]	0.65	5.11	14.45
10	[13,15,6,5,9,0,4,12,3,10,2,7,1,8,11,14]	0.89	5.94	16.14

As evidenced by the table, except for Solutions 1, 2, 3 and 8 which do not simultaneously outperform the original scenario in both production capacity and energy consumption, all other solutions demonstrate higher production capacity and lower energy consumption compared to the baseline.

7. Conclusions and future work

In this paper, we address the circular layout problem of intelligent production units with AGV transportation, and establish a multi-objective mixed-integer linear programming model. A genetic algorithm incorporating fast non-dominated sorting is used for solving this multi-objective problem, and the algorithm is improved by introducing isomorphism processing of directed graphs which accurately expresses the characteristics of the layout problem. The production organization method of intelligent units is reflected in the simulation black box. Simulation experimental methods can better describe the problem characteristics of intelligent units, allowing for a more accurate assessment of the objective function values, though at a slower speed. Using a typical workshop of an intelligent production unit as an example, several sets of simulation optimization experiments were designed. The results indicate that isomorphism processing can effectively reduce the search time of the optimization algorithm and improve the quality of the solutions, thereby validating the effectiveness and superiority of the algorithm.

In future research, to significantly improve optimization speed, subsequent research will adopt queue network modeling to solve performance indicators, replacing simulation for performance metrics. Additionally, beyond circular layouts, the study will further explore different types of unit layouts.

Funding

This work was supported by the Guangdong Basic and Applied Basic Research Foundation of China [grant numbers 2025A1515010208; 2024A1515010906], and the National Natural Science Foundation of China [grant number 72202044].

References

- Amar, S. H., & Abouabdellah, A. (2016, November). Facility layout planning problem: Effectiveness and reliability evaluation system layout designs. *In 2016 International Conference on System Reliability and Science (ICSRS) (pp. 110-114)*. IEEE.
- Azadivar, F., & Wang, J. (2000). Facility layout optimization using simulation and genetic algorithms. *International Journal of Production Research*, 38(17), 4369-4383.
- Azimi, P., & Saberi, E. J. E. C. (2013). An efficient hybrid algorithm for dynamic facility layout problem using simulation technique and pso. *Economic Computation & Economic Cybernetics Studies & Research*, 47(4).
- Bányai, T. (2023). Energy efficiency of AGV-drone joint in-plant supply of production lines. *Energies*, 16(10), 4109.
- Castillo, I., & Peters, B. A. (2004). Integrating design and production planning considerations in multi-bay manufacturing facility layout. *European Journal of Operational Research*, 157(3), 671-687.
- Chen, G. Y. H., & Lo, J. C. (2014). Dynamic facility layout with multi-objectives. *Asia-Pacific Journal of Operational Research*, 31(04), 1450027.
- Chen, G. Y., & Rogers, K. J. (2009, December). Proposition of two multiple criteria models applied to dynamic multi-objective facility layout problem based on ant colony optimization. *In 2009 IEEE International Conference on Industrial Engineering and Engineering Management (pp. 1553-1557)*. IEEE.
- Deb, K., Pratap, A., Agarwal, S., & Meyarivan, T. A. M. T. (2002). A fast and elitist multiobjective genetic algorithm: NSGA-II. *IEEE transactions on evolutionary computation*, 6(2), 182-197.
- Derakhshan Asl, A., & Wong, K. Y. (2017). Solving unequal-area static and dynamic facility layout problems using modified

- particle swarm optimization. *Journal of Intelligent Manufacturing*, 28(6), 1317-1336.
- Drira, A., Pierreval, H., & Hajri-Gabouj, S. (2007). Facility layout problems: A survey. *Annual reviews in control*, 31(2), 255-267.
- Dunker, T., Radons, G., & Westkämper, E. (2005). Combining evolutionary computation and dynamic programming for solving a dynamic facility layout problem. *European Journal of Operational Research*, 165(1), 55-69.
- Durmaz, E. S. R. A., & Şahin, R. A. M. A. Z. A. N. (2017). NSGA-II and goal programming approach for the multi-objective single row facility layout problem. *Journal of the Faculty of Engineering and Architecture of Gazi University*, 32(3).
- Erik, A., & Kuvvetli, Y. (2021). Integration of material handling devices assignment and facility layout problems. *Journal of Manufacturing Systems*, 58, 59-74.
- Ferretti, I., Zaroni, S., & Zavanella, L. E. (2023). Facility layout problem with auxiliary systems for energy efficiency. *International Journal of Systems Science*, 54(14), 2799-2808.
- Fragapane, G., Ivanov, D., Peron, M., Sgarbossa, F., & Strandhagen, J. O. (2022). Increasing flexibility and productivity in Industry 4.0 production networks with autonomous mobile robots and smart intralogistics. *Annals of operations research*, 308(1), 125-143.
- Guo, W., Jiang, P., & Yang, M. (2023). Unequal area facility layout problem-solving: a real case study on an air-conditioner production shop floor. *International Journal of Production Research*, 61(5), 1479-1496.
- Huo, J., Liu, J., & Gao, H. (2021). An nsga-ii algorithm with adaptive local search for a new double-row model solution to a multi-floor hospital facility layout problem. *Applied Sciences*, 11(4), 1758.
- Jithavech, I., & Krishnan, K. K. (2010). A simulation-based approach for risk assessment of facility layout designs under stochastic product demands. *The International Journal of Advanced Manufacturing Technology*, 49(1), 27-40.
- Johnson, D. S., & Garey, M. R. (1979). Computers and intractability: A guide to the theory of NP-completeness. *WH Freeman*: 208-209.
- Kheirkhah, A., Navidi, H., & Bidgoli, M. M. (2015). Dynamic facility layout problem: a new bilevel formulation and some metaheuristic solution methods. *IEEE Transactions on Engineering Management*, 62(3), 396-410.
- Klausnitzer, A., & Lasch, R. (2019). Optimal facility layout and material handling network design. *Computers & Operations Research*, 103, 237-251.
- Koren, Y. (2019). Reconfigurable manufacturing system. In *CIRP Encyclopedia of Production Engineering* (pp. 1417-1423). Springer, Berlin, Heidelberg.
- Kubalík, J., Kurilla, L., & Kadera, P. (2023). Facility layout problem with alternative facility variants. *Applied Sciences*, 13(8), 5032.
- Li, Y., & Li, Z. (2023). Bi-objective optimization for multi-row facility layout problem integrating automated guided vehicle path. *IEEE Access*, 11, 55954-55964.
- Lin, L. C., & Sharp, G. P. (1999). Quantitative and qualitative indices for the plant layout evaluation problem. *European Journal of Operational Research*, 116(1), 100-117.
- Liu, Z., Guo, S., & Wang, L. (2019). Integrated green scheduling optimization of flexible job shop and crane transportation considering comprehensive energy consumption. *Journal of cleaner production*, 211, 765-786.
- Loiola, E. M., De Abreu, N. M. M., Boaventura-Netto, P. O., Hahn, P., & Querido, T. (2007). A survey for the quadratic assignment problem. *European journal of operational research*, 176(2), 657-690.
- Ma, H., Zhang, Y., Sun, S., Liu, T., & Shan, Y. (2023). A comprehensive survey on NSGA-II for multi-objective optimization and applications. *Artificial Intelligence Review*, 56(12), 15217-15270.
- Mittal, S., Khan, M. A., Romero, D., & Wuest, T. (2019). Smart manufacturing: Characteristics, technologies and enabling factors. *Proceedings of the Institution of Mechanical Engineers, Part B: Journal of Engineering Manufacture*, 233(5), 1342-1361.
- Mohammed, M. A. and R. A. Hasan (2017). Particle swarm optimization for facility layout problems FLP - A comprehensive study. *IEEE International Conference on Intelligent Computer Communication and Processing ICCP, IEEE; Tech Univ Cluj Napoca, Dept Comp Sci; Tech Univ Cluj Napoca; Acad Tech Sci Romania; IEEE Romania Sect; Robert Bosch SRL; Porsche Engn Romania SRL*: 93-99.
- Nguyen, K. D., Tran, T. T., & Vo, D. N. (2026). An efficient Salp Swarm Algorithm for optimizing wind farm layouts with neighboring farm impacts. *International Journal of Green Energy*, 23(2), 420-435.
- Peng, Y., Zeng, T., Fan, L., Han, Y., & Xia, B. (2018). An improved genetic algorithm based robust approach for stochastic dynamic facility layout problem. *Discrete Dynamics in Nature and Society*, 2018(1), 1529058.
- Pérez-Gosende, P., Mula, J., & Díaz-Madroñero, M. (2021). Facility layout planning. An extended literature review. *International Journal of Production Research*, 59(12), 3777-3816.
- Phoon, S. Y., Yap, H. J., Taha, Z., & Pai, Y. S. (2017). Interactive solution approach for loop layout problem using virtual reality technology. *The International Journal of Advanced Manufacturing Technology*, 89(5), 2375-2385.
- Pourhassan, M. R., & Raissi, S. (2017). An integrated simulation-based optimization technique for multi-objective dynamic facility layout problem. *Journal of Industrial Information Integration*, 8, 49-58.
- Rezazadeh, H., Ghazanfari, M., Saidi-Mehrabad, M., & Jafar Sadjadi, S. (2009). An extended discrete particle swarm optimization algorithm for the dynamic facility layout problem. *Journal of Zhejiang University-Science A*, 10(4), 520-529.
- Samarghandi, H., Taabayan, P., & Jahantigh, F. F. (2010). A particle swarm optimization for the single row facility layout problem. *Computers & Industrial Engineering*, 58(4), 529-534.
- Schudeleit, T., Züst, S., Weiss, L., & Wegener, K. (2016). The total energy efficiency index for machine tools. *Energy*, 102,

- Sedehi, M. S., & Farahani, R. Z. (2009). An integrated approach to determine the block layout, AGV flow path and the location of pick-up/delivery points in single-loop systems. *International Journal of Production Research*, 47(11), 3041-3061.
- Shang, L., Liu, B., & Peng, R. (2025). Designing random collaborative warranty and customizing maintenance strategies for systems subject to mission cycles. *Reliability Engineering & System Safety*, 257, 110843.
- Singh, S. P., & Sharma, R. R. (2006). A review of different approaches to the facility layout problems. *The International Journal of Advanced Manufacturing Technology*, 30(5), 425-433.
- Tayal, A., Gunasekaran, A., Singh, S. P., Dubey, R., & Papadopoulos, T. (2017). Formulating and solving sustainable stochastic dynamic facility layout problem: A key to sustainable operations. *Annals of Operations Research*, 253(1), 621-655.
- Urban, T. L. (1998). Solution procedures for the dynamic facility layout problem. *Annals of operations research*, 76, 323-342.
- Wang, G., Yan, Y., Zhang, X., Shangguan, J., & Xiao, Y. (2008, December). A simulation optimization approach for facility layout problem. In *2008 IEEE International Conference on Industrial Engineering and Engineering Management (pp. 734-738)*. IEEE.
- Yao, Y., Li, X., & Gao, L. (2024). A DQN-based memetic algorithm for energy-efficient job shop scheduling problem with integrated limited AGVs. *Swarm and Evolutionary Computation*, 87, 101544.
- Ye, M., & Zhou, G. (2007). A local genetic approach to multi-objective, facility layout problems with fixed aisles. *International Journal of Production Research*, 45(22), 5243-5264.
- Yue, L., Fan, H., & Zhai, C. (2019). Joint configuration and scheduling optimization of a dual-trolley quay crane and automatic guided vehicles with consideration of vessel stability. *Sustainability*, 12(1), 24.
- Zarea Fazlelahi, F., Pournader, M., Gharakhani, M., & Sadjadi, S. J. (2016). A robust approach to design a single facility layout plan in dynamic manufacturing environments using a permutation-based genetic algorithm. *Proceedings of the institution of mechanical engineers, Part B: journal of engineering manufacture*, 230(12), 2264-2274.
- Zha, S., Guo, Y., Huang, S., Wu, Q., & Tang, P. (2020). A hybrid optimization approach for unequal-sized dynamic facility layout problems under fuzzy random demands. *Proceedings of the Institution of Mechanical Engineers, Part B: Journal of Engineering Manufacture*, 234(3), 382-399.
- Zhang, H. Y., Li, H., Liang, Z. P., Xi, S. H., & Wang, X. (2025). Performance analysis of an intelligent manufacturing cell with multi-resource collaboration. *International journal of industrial engineering computations*, 16(4), 1155-1176.
- Zhang, L., Yan, Y., & Hu, Y. (2024). Deep reinforcement learning for dynamic scheduling of energy-efficient automated guided vehicles. *Journal of Intelligent Manufacturing*, 35(8), 3875-3888.
- Zhang, Y., Zhang, H., Xia, M. M., Lu, T. T., & Jiang, L. L. (2009, July). Research on applying unidirectional loop layout to optimize facility layout in workshop based on improved genetic algorithm. In *2009 IITA International Conference on Control, Automation and Systems Engineering (case 2009) (pp. 144-147)*. IEEE.
- Zhao, Y., Lu, J., & Yi, W. (2020). A new cellular manufacturing layout: Multi-floor linear cellular manufacturing layout. *International Journal of Advanced Robotic Systems*, 17(3), 1729881420925300.
- Zhou, L., Li, J., Li, F., Meng, Q., Li, J., & Xu, X. (2016). Energy consumption model and energy efficiency of machine tools: a comprehensive literature review. *Journal of Cleaner Production*, 112, 3721-3734.
- Zouein, P. P., & Kattan, S. (2022). An improved construction approach using ant colony optimization for solving the dynamic facility layout problem. *Journal of the Operational Research Society*, 73(7), 1517-1531.

